

# Journal of Rehabilitation in Civil Engineering

Journal homepage: https://civiljournal.semnan.ac.ir/

# Enhancing High-Modulus Asphalt Mixture Performance: The Role of Nano-ZnO and SBS Additives in Bitumen Modification

# Shahram Naseri <sup>1</sup>, Gholamali Shafabakhsh <sup>2,\*</sup>; Alireza Khavandi <sup>3</sup>

- 1. Ph.D. Candidate, Department of Civil Engineering, Faculty of Engineering, University of Semnan, Semnan, Iran
- 2. Professor, Department of Civil Engineering, Faculty of Engineering, University of Semnan, Iran
- 3. Associate Professor, Department of Civil Engineering, Faculty of Engineering, University of Zanjan, Zanjan, Iran
- \* Corresponding author: ghshafabakhsh@semnan.ac.ir

#### **ARTICLE INFO**

# Article history:

Received: 29 April 2025 Revised: 31 July 2025 Accepted: 17 August 2025

Keywords: High-modulus mixture; Nano-ZnO; Styrene-butadiene-styrene; Low-temperature cracking; Gap-graded.

# **ABSTRACT**

This study explores enhancing high-modulus asphalt mixture (HMAM) performance with commonly used bitumen with a penetration grade of 60/70 instead of a low penetration grade. To achieve the desired stiffness and mitigate thermal cracking, three dosages of 3.5, 4.2, and 4.9% of zinc oxide (Nano-ZnO) and three dosages of 3.2, 3.7, 4.2% of styrenebutadiene-styrene (SBS) were incorporated as additives. Comprehensive performance tests were conducted, including BBR, LAS, and MSCR for bitumen, alongside low-temperature SCB and moisture susceptibility tests for the asphalt mixture. Statistical analysis using one-way ANOVA was performed to validate the results. The findings revealed that gapgraded asphalt mixtures alone did not yield HMAM; however, Nano-ZnO (3.5, 4.2, and 4.9%) and SBS (3.2, 3.7, and 4.2%) additives significantly improved dynamic modulus and produced HMAM. Based on the flexural creep stiffness and m-value results, the modified bitumen ones exhibited superior low-temperature performance; generally, at least improvement in mixture performance has been achieved. Moreover, these additives improved damage resistance and fatigue performance, which can be interpreted by demonstrating enhanced orderliness and reduced polar component accumulation. Elastic recovery and non-recoverable creep compliance were notably improved through the modification process, indicating better resistance to both elastic and permanent deformations. Additionally, the modifications enhanced fracture properties and moisture resistance. The optimal percentages for Nano-ZnO and SBS are suggested to be 4.2% and 3.2%, respectively, underscoring their significant benefits in enhancing the performance of HMAM by improving the physical properties of bitumen, reducing its solubility parameter, and increasing compatibility with SBS.

E-ISSN: 2345-4423

© 2025 The Authors. Journal of Rehabilitation in Civil Engineering published by Semnan University Press. This is an open access article under the CC-BY 4.0 license. (https://creativecommons.org/licenses/by/4.0/)

#### How to cite this article:

Naseri, S., Shafabakhsh, G. and Khavandi, A. (2026). Enhancing High-Modulus Asphalt Mixture Performance: The Role of Nano-ZnO and SBS Additives in Bitumen Modification. Journal of Rehabilitation in Civil Engineering, 14(2), 2328 <a href="https://doi.org/10.22075/jrce.2025.2328">https://doi.org/10.22075/jrce.2025.2328</a>

## 1. Introduction

High Modulus Asphalt Mixtures (HMAM) have become a promising solution in asphalt pavement engineering. They were initially introduced to reduce the thickness of base layers and subsequently utilized in binder and coating layers to improve rutting resistance under heavy traffic conditions [1–4]. By following aggregate packing principles, HMAM with dense-graded or gap-graded skeletons demonstrates excellent load-bearing capacity, as shown in various studies [5-9]. Their improved load absorption and high complex modulus help reduce strain within the pavement structure, enabling a significant reduction in pavement thickness by 20%-30% [8,10]. Moreover, outperforms conventional mixtures in rutting resistance, even surpassing those modified with polymeric bitumen, thereby increasing the pavement's fatigue life [11–13]. Concurrently, EME2 technology, originating in France in the early 1990s, presents another milestone [6]. Named "enrobes module eleve" or "high-modulus asphalt," EME2 employs lowpenetration grade bitumen, i.e., 10-35, and high bitumen content, approximately 6%, to enhance its fatigue resistance [14]. EME2 was also introduced into Queensland through a joint initiative among various companies [10]. Studies have shown that the decrease in thickness achieved with the interim procedure is consistent with the anticipated reductions outlined in the complete French methodology compared to traditional asphalt mixes. Further innovations, such as grave bitumen Class 5 (GB5), refined by Pouget et al. [15], optimize aggregate gradation and bitumen content for superior performance. GB5 followed Aggregate Packing theory and used single or double-gap-graded curves to improve aggregate interlocking. Moreover, low-penetration bitumen was used to generate this mixture. Therefore, highperformance features were obtained for GB5 incorporating a low bitumen content, typically around 4% to 4.5% by total weight [16]. Lee et al. assessed the performance of HMAM in flexible pavement rehabilitation [17]. Their research compared the durability and mechanical properties of HMAM and conventional asphalt mixtures through laboratory tests and field evaluations. HMAM proved effective in reducing pavement distress and improving the overall condition of flexible pavements, which can lower maintenance costs and extend pavement service life.

Huang et al. investigated the characteristics of HMAM, focusing specifically on their application in heavy traffic pavements [17]. This study covered aspects such as mixture design, mechanical properties, and rutting resistance, providing insights into the suitability of HMAM for pavements exposed to high traffic loads. By optimizing the mixture design, HMAM demonstrated potential in enduring heavy traffic loads and sustaining long-term pavement performance within high-volume traffic environments. Another study investigated how HMAM performed in cold climates, where pavements faced freezing and thawing cycles [18]. Through laboratory tests and field observations, the research found that HMAM displayed better resistance to cracking and rutting compared to traditional asphalt mixtures in cold weather conditions. Different aggregate types, binder modifications, and additives were assessed to enhance HMAM's durability and performance such climates. Overall, the findings indicated that HMAM holds strong potential for increasing pavement longevity and minimizing maintenance costs in cold regions. Recently, in the study of Khiavi et al., the behavior of conventional asphalt mixtures and HMAM (EME2 and GB5) was examined [18]. The results indicated that using hard-penetration bitumen in HMAM (EME2 and GB5) as a surfacing material provides notable advantages over conventional mixtures, particularly in terms of mechanical performance and durability.

Moreover, recent studies combining experimental and molecular dynamics approaches have demonstrated that nanoscale additives can significantly enhance the mechanical performance of composite materials. Nevertheless, the reliance on low-penetration or hard-grade bitumen introduces certain limitations, especially regarding low-temperature cracking and material availability in many regions. To address these challenges, the current study proposes an alternative approach by utilizing 60/70 penetration grade bitumen, which is more commonly available in the pavement industry, combined with appropriate modifications. Specifically, SBS polymer and Nano-ZnO additives were used to transform conventional

60/70 bitumen into a high-performance binder suitable for HMAM, similar to those used in GB5. This strategy aims to maintain the structural benefits of HMAM, while enhancing low-temperature performance and providing a more practical, cost-effective solution for regions where low-penetration bitumen is scarce or expensive. Therefore, this research focuses on developing a modified HMAM using 60/70 bitumen, combined with Nano-ZnO and SBS additives, alongside a GB5-inspired gradation curve. The study evaluates key performance aspects, including stiffness, rutting resistance, and fatigue behavior, while addressing low-temperature cracking concerns traditionally associated with HMAM. An overall flowchart of the process carried out in this research has been presented in Fig. 1.

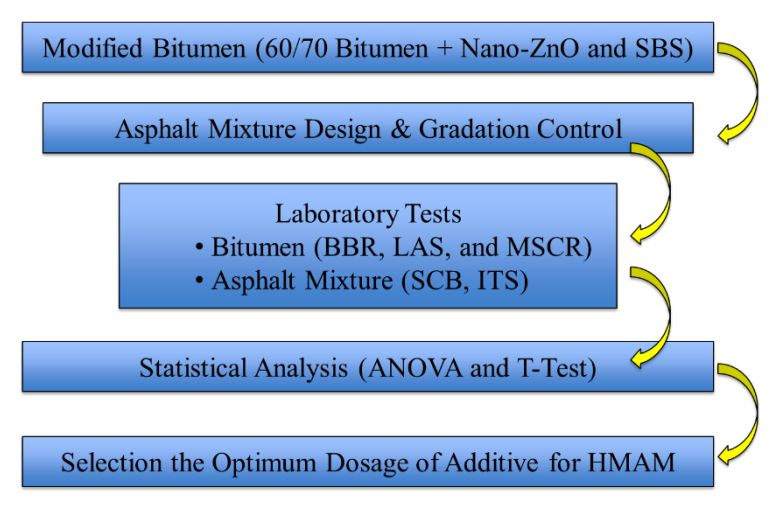


Fig. 1. Schematic flowchart of the research process.

# 2. Experimental program

#### 2.1. Materials

# 2.1.1. Additives

Styrene-butadiene-styrene (SBS) and Zinc Oxide (Nano-ZnO) are the two selected additives used in this study. The benefits of these additives, such as improvement in rutting, fatigue, and low-temperature cracking resistance in asphalt mixture, were the reasons for this selection [19,20]. Physical and chemical characteristics of these nano materials are provided in Table 1.

Nano-Zno	)	SBS			
Properties	Quantety	Properties	Quantety		
Molecular formula	0	Structures	Linear		
$SSA(m^2/g)$	> 35	S/B (mass ratio)	30/70		
Crystallite size (nm)	30	Tensile strength (MPa)	15.0		
Purity (%)	95	Tensile elongation (%)	700		
Color	Light yellow	300% constant stress (MPa)	2.0		
Crystal form	Rutile type	Tensile permanent deformation (%)			

**Table 1.** Characteristics of addetives used in this study.

Moreover, as mentioned, it is tried to fabricate a low-penetration grade bitumen from a commonly used bitumen in the pavement industry, i.e., 60/70 (PG64-16), with appropriate additives to generate a high-modulus mixture. This grade of bitumen was provided by related work with a low penetration of the original bitumen, e.g., PG70-10. The modification process is considered to eliminate the challenges of HMHMA, especially cracking at low temperatures.

#### 2.1.2. Bitumen

This study utilized a bitumen with a penetration grade of 60/70 (PG 64-16). The classical specifications for neat bitumen and modified bitumen are detailed in Table 2. The selected dosage ranges of Nano-ZnO (3.5%–4.9%) and SBS (3.2%–4.2%) were determined based on relevant technical literature [21–25] ensuring compatibility with the base 60/70 bitumen and alignment with typical modification levels used in similar studies.

The incorporation of additives, including SBS and Nano-ZnO, was performed using a high-shear mixer at 4000 rpm for 60 minutes, following the protocols recommended in prior studies [19,20]. The mixing temperature was maintained at  $180 \pm 5^{\circ}$ C to ensure homogenous dispersion of the additives within the bitumen matrix. Scanning Electron Microscopy (SEM) are typically recommended, because of constraints in the limitations, an alternative practical approach was adopted. A cylindrical sample of the modified binder was prepared, and samples were extracted from the upper, central, and lower portions of the cylinder. These samples were then subjected to softening point and penetration tests. As reported by AASHTO 1993 [26], the differences in test results across these sections must remain within an acceptable range to confirm uniform dispersion of the modifiers. In all modified binder samples, the variation remained within the permissible limits, confirming adequate mixing quality.

Table 2. Labeling system of different bitumen types and their properties

Sample Code	Nano-ZnO Content (% by total weight.)	SBS Content (% by total weight.)	Penetration Value (0.1 mm)	Softening Point (°C)
N	0	0	68	49
T1	3.5	0	63	54
T2	4.2	0	62	56
Т3	4.9	0	59	58
T4	3.5	3.2	56	62
T5	3.5	3.7	54	64
Т6	3.5	4.2	52	65
Т7	4.2	3.2	54	66
Т8	4.2	3.7	51	67
Т9	4.2	4.2	49	70
T10	4.9	3.2	52	69
T11	4.9	3.7	49	73
T12	4.9	4.2	47	78

# 2.1.3. Aggregate

The asphalt mixture samples were fabricated using limestone aggregate. The gradation curve was based on the aggregate packing theory and the experiences obtained by Olard et al. in France [7]. According to their recommendations, the filler content in the asphalt mixture must be controlled. In summary, the present research used a gap-graded mixture containing aggregates up to a maximum size of 19 mm. Fig. 2 shows the optimized gradation. The upper and lower limites of this gradation are provided in accordance with Iran's Highway Asphalt Paving Code, Publication No. 234 [27].

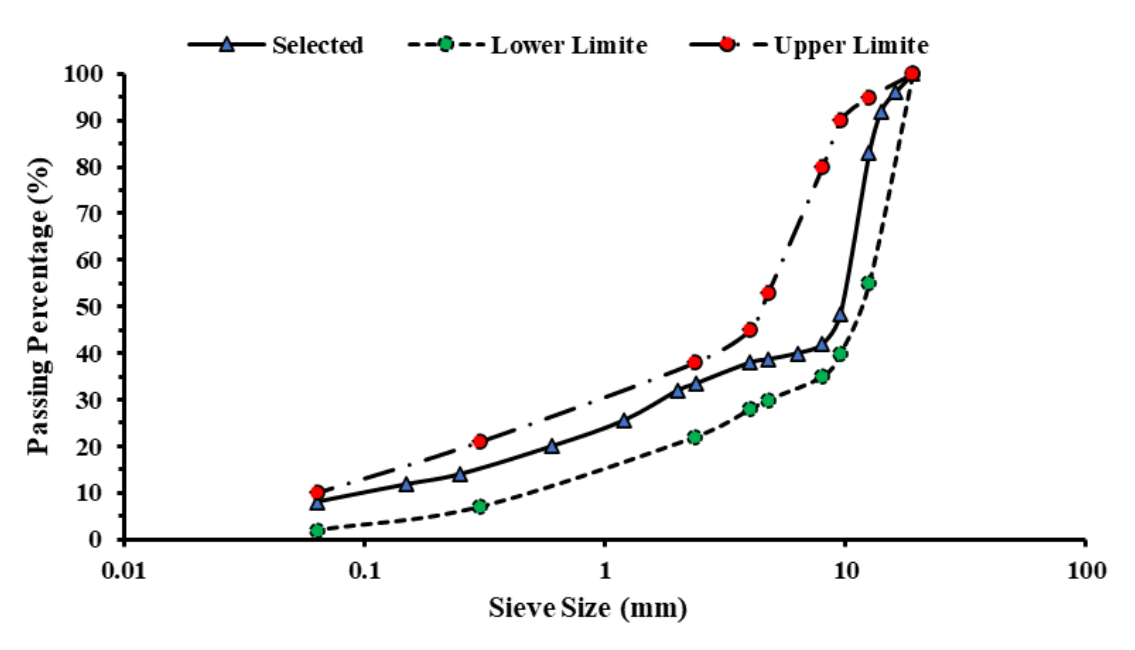


Fig. 2. The gap-graded curves used in this study.

## 2.2. Test method

## 2.2.1. Mix design

In accordance with the ASTM D1559 [28], Marshall samples were prepared using bitumen contents of 3.0%, 3.5%, 4.0%, 4.5%, 5.0%, and 5.5%. To simulate traffic loading, each sample was compacted by applying 50 blows per side. After verifying compliance with the standard specifications, the optimal bitumen content for the control asphalt mixture was found to be 4.2 percent. This bitumen percentage was also applied to modified asphalt mixtures, and all mix design parameters were controlled.

#### 2.2.2. Bitumen tests

# 2.2.2.1. Aging procedure

The short-term laboratory aging of the bitumen was performed using the rolling thin-film oven test (RTFOT) according to ASTM D2872 [29]. Additionally, based on ASTM D6521, a pressure-aging vessel (PAV) was implemented at 100°C for 20 hours subjected to 2 MPa of pressure [30].

#### 2.2.2.2. Bending beam rheometer test

The main results of the bending beam rheometer (BBR) test are flexural creep stiffness, S(t), and the stress relaxation rate, m-value. Through the application of a localized force of  $980 \pm 50$  mN at the midpoint of a prismatic specimen and measuring the deflection at this point can determine these parameters over 240 seconds with a time step of 0.5 seconds [31]. To determine the flexural creep stiffness, S(t), the elastic-viscoelastic correspondence principle should be used [32–34] as Eq. (1):

$$S_{(t)} = \frac{P \times L^3}{4 \times b \times h^2 \times \delta_{(t)}} \tag{1}$$

where  $\delta_{(t)}$  represents the deflection of the beam at midspan (mm); P is the applied constant load (N); L denotes the span length (mm); b and h are the width and depth of the beam (mm), respectively; and t is the time (s). The creep rate, or m-value, is the absolute value of the slope of the  $\log(S_{(t)})$  -  $\log(t)$  curve, determined by Eq. (2):

$$m_{(t)} = \left| \frac{d \log(S_{(t)})}{d \log(\delta_{(t)})} \right| \tag{2}$$

The BBR test was conducted at temperatures 0, -6, -12, -18, and -24°C following the ASTM D6648 standard[29]. The master curve of creep stiffness versus time, along with the two Superpave control parameters, S(t) and m-Value, will be used as the test's outputs to analyze the results.

## 2.2.2.3. LAS test

The linear amplitude sweep test (LAS) is one of the preferred tests for determining the fatigue of bitumen. This test, conducted according to the AASHTO-TP-101-14 standard [35] evaluates the fatigue of unmodified and modified bitumen.

In this study, the Dynamic Shear Rheometer (DSR) was used to characterize bitumen obtained from Pressure Aging Vessel (PAV) tests [30]. An 8-mm-wide circular plate with a 2 mm gap was employed for all samples. Initially, a frequency sweep testing was executed at 0.1% strain across an intermediate Superpave temperature of  $25^{\circ}$ C ( $\frac{(64-22)}{2}+4=25$ ), spanning frequencies from 0.1 to 100 Hz. Subsequently, specimens were stabilized for 10 minutes at a specific temperature selected from the intermediate range. To assess the bitumen's properties in an undamaged state, another frequency sweep test was performed at a strain level of 0.1% over a frequency range of 0.1–30 Hz. The damage parameter,  $\alpha$ , was determined by employing the slope derived from a log-log graph of storage modulus (G') versus angular frequency ( $\omega$ ) based on the undamaged rheological properties. Following the frequency sweep tests, a linear amplitude sweep was performed at the temperature selected for the test. This process consisted of imposing oscillatory shear under strain-controlled conditions at a fixed frequency of 10 Hz. The test comprised 31 intervals, each lasting 10 seconds. The initial interval started at 0.1% strain, with subsequent intervals increasing at a constant rate of 1%, culminating at 30% strain.

The LAS test is capable of prediction of bitumen fatigue life in relation to applied strain within pavements. The analysis of the results requires the governing Eq.s of viscoelastic continuum damage (VECD), which are briefly presented below:

The results of the frequency sweep test are utilized to derive the damage parameter  $\alpha$ , which is a function of the slope G' (storage modulus) and  $\omega$  (angular frequency), where G' can be calculated using Eq. (3):

$$G'(\omega) = \left| G^*_{(\omega)} \right| \times \cos(\delta(\omega)) \tag{3}$$

Subsequently,  $\alpha$  was calculated as the gradient inverse of the log(G') versus log( $\omega$ ) plot based on Eq. (4):

$$log[G'(\omega)] = m \times log(\omega) + b = \frac{1}{\alpha} \times log(\omega) + b$$
(4)

Accumulated damage ( $D_{(t)}$ ), indicating the asphalt binder's susceptibility to fatigue distress, was computed using Eq. (5) and Eq. (6):

$$D_{(t)} = \sum_{i=1}^{n} \left[ \prod \gamma_0^2 (C_{i-1} - C_i) \right]^{\frac{\alpha}{1+\alpha}} \times (t_i - t_{i-1})^{\frac{1}{1+\alpha}}$$
 (5)

$$C_i = \frac{|G^*| \times \sin(\delta_{(t)})}{|G_0^*| \times \sin(\delta_{initial})} \tag{6}$$

Here,  $\gamma^2_0$  represents the imposed strain corresponding to a particular data point of  $C_i$ ;  $|G^*|$  denotes the complex shear modulus in MPa,  $\alpha$  is the aforementioned damage parameter, and t stands for time in seconds.

At each time-specific data point,  $G^*$ .sin  $\delta_{(t)}$  and  $D_{(t)}$  can be calculated. It is considered that  $C_0$  equals 1 at  $D_{(0)}$ , with  $D_{(0)}$  being 0. Eq. (7) illustrates the connection between C and  $D_{(t)}$ , with the parameters  $C_0$ ,  $C_1$ , and  $C_2$  determined through a straightforward curve-fitting process involving power law functions.

$$C = C_0 - C_1 \times (D_{(t)})^{C_2} \tag{7}$$

 $D_f$  (the value of  $D_{(t)}$  at failure) is defined as the point where the fatigue parameter ( $|G^*|\sin\delta$ ) decreases by 35% from its initial value. Eq. (8) was employed to calculate  $D_f$ .

$$D_f = 0.35 \times \left(\frac{c_0}{c_1}\right)^{\frac{1}{c_2}} \tag{8}$$

Two model parameters, A and B, are necessary to assess the fatigue performance parameter of the asphalt binder (N<sub>f</sub>). These parameters (A and B) are determined as follows, where f represents the loading frequency (10 Hz), I<sub>D</sub> is the average of shear modulus during the strain of 1%, and  $k = 1 + (1-C_2)^{\alpha}$ :

$$A = \frac{f(D_f)^k}{k(\pi I_D C_1 C_0)^\alpha} \tag{9}$$

$$B = 2 \times \alpha \tag{10}$$

Finally, the asphalt binder's fatigue parameter ( $N_f$ ) is computed using Eq. (11), where  $\gamma_{max}$  signifies the highest anticipated strain of asphalt binder for a particular pavement structure.

$$N_f = A \times (\gamma_{\text{max}}) - B \tag{11}$$

#### 2.2.2.4. MSCR test

The mean non-recoverable creep compliance ( $J_{nr}$ ) and the mean percentage of recoverable strain (R%) are two primary parameters derived from the Multiple Stress Creep and Recovery (MSCR) test to assess the irreversible deformation of bitumen. According to ASTM D7405 [30] and Eq. (12),  $J_{nr}$  under each loading level ( $J_{nr(\sigma)}$ ) is calculated by dividing the mean non-recoverable strain ( $\xi_{10}$ ) from 10 creep and recovery cycles by the applied stress ( $\sigma$ ) during those cycles. This test was performed on RTFO-bitumen at three different temperatures of 58°C, 64°C, and 70°C.

$$J_{nr(\sigma)} = \frac{\sum_{n=1}^{10} J_{nr(\sigma,n)}}{10} = \frac{\sum_{n=1}^{10} \frac{\xi_{10}}{\sigma}}{10}$$
 (12)

Also, the recovery percentage (R%) can be calculated as Eq. (13):

$$R_{(\sigma)} = \frac{\sum_{n=1}^{10} \xi_{r(\sigma,n)}}{10} = \frac{\sum_{n=1}^{10} \frac{(\xi_c - \xi_0 - \xi_{10}) \times 100}{(\xi_c - \xi_0)}}{10}$$
(13)

In which  $\xi_C$  is the terminal strain value observed after creep in every cycle, and  $\xi_0$  is the strain observed at the start of the creep period for every cycle.

#### 2.2.3. Mixture tests

## 2.2.3.1. Dynamic modulus test

The standard AASHTO T342-11 [36] was used to measure the dynamic modulus of asphalt mixtures to determine whether a high dynamic modulus asphalt mixture was produced. According to the definition of French specification (Capitão and Picado-Santos) [37], the HMAM at a temperature of 15°C and a frequency of 10 Hz should have a minimum dynamic modulus of 14,000 MPa. Therefore, this test was conducted under the conditions mentioned in the asphalt samples using the UTM device.

#### 2.2.3.2. Semi-circular bending test

The Semi-Circular Bending (SCB) test is a fracture-based test geometry, and the specimen can be obtained from laboratory-compacted or field-cored samples. A small notch is inserted on the straight edge, and the specimen would be ready to loaded. The concept of elasticity is employed to explain stress-displacement in the vicinity of the tip of the crack, assuming isotropic, homogeneous, and elastic material characteristics assuming a plane stress scenario. The SCB test is applicable for assessing the low-temperature behavior of asphalt mixtures.

A Stress Intensity Factor (SIF) represents the stress distribution surrounding the crack tip in a linearly elastic medium under mode I fracture conditions. As the stress nears failure at the crack tip, the Stress Intensity Factor (SIF) reaches a critical point referred to as fracture toughness (K<sub>c</sub>). This parameter characterizes the stress concentration around the crack tip and the capacity of the material to withstand crack formation. For mode I fracture, this parameter is computed as Eq. (14) [38]:

$$K_{IC} = \sigma_{0C} \times \sqrt{\pi a} \times Y_I \tag{14}$$

The Eq. can be expressed as  $\sigma_{0c} = P/2rt$ , where  $Y_I$  represents the normalized SIF, r denotes the specimen's radial dimension, t signifies the specimen thickness, P stands for the fracture load, and a represents the crack length (induced notch).

Li and Marasteanu [39] utilized acoustic emissions to establish that, in SCB specimens, the fracture process zone spans approximately 3–6 mm in width and 20–30 mm in length. Their findings led them to conclude that Linear Elastic Fracture Mechanics (LEFM) assumptions do not apply to this geometry size and that fracture toughness does not accurately represent a material parameter. Fracture energy (G<sub>f</sub>) is a fracture parameter that depends less on LEFM assumptions and material homogeneity compared to fracture toughness. This property is not affected by specimen size or shape and represents the energy needed for a crack to grow. It is especially appropriate for use with asphalt concrete, a material classified as quasi-brittle yet demonstrating ductile fracture behavior. According to Eq. (15), fracture energy can obtained in accordance with the RILEM TC50-FMC specifications [40] by dividing the area under the load-deflection response curve (fracture work) by the ligament's cross-sectional area. To compute the ligament area, the ligament length is multiplied by the thickness of the specimen.

$$G_f = \frac{W_0 + mg\delta_0}{A_{lig}} \tag{15}$$

 $W_0$  represents the total work, with m denoting the specimen's mass, g representing the acceleration due to gravity (9.81 m/s<sup>2</sup>),  $A_{lig}$  indicating the ligament's area, and  $\delta_0$  denoting the deformation reached at the point of final failure of the specimen. Cylindrical hot-mix asphalt samples (150 mm  $\times$  150 mm), compacted via a gyratory method, were sectioned to produce SCB test specimens. The four SCB samples shown in Fig. 3 were obtained from the central part of the cylindrical specimens. The previous numerical studies of SCB samples with 25 mm and 50 mm thicknesses revealed that the stresses along the thickness axis were negligible, supporting the application of plane stress analysis for the 25 mm sample [39]. This characteristic is crucial for conducting fracture tests on laboratory samples. A 25-mm-thick SCB sample with a 15-mm-deep and 2-mm-wide notch was utilized, in line with previous research [41,42].

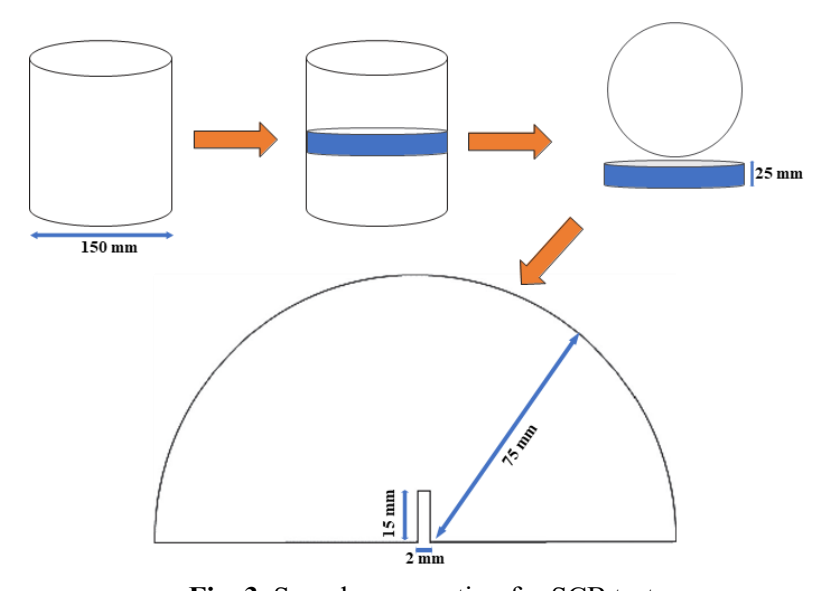


Fig. 3. Sample preparation for SCB test.

A 10 kN universal testing machine was employed to load specimens, which were supported between two rollers separated by 120 mm. The specimens were subjected to three-point loading at a constant rate of 0.01 mm/s at temperatures of -20, -15, and -5°C. Measurements of load and displacement continued until the specimens fractured.

#### 2.2.3.3. ITS test

The investigation into moisture damage in Marshall samples with a 7% air void was conducted using the modified Latman standard AASHTO T283 [43]. The samples were divided into conditioned and unconditioned sets, with the conditioned samples being subjected to a freezing-thaw cycle. Subsequently, the moisture durability of the samples was evaluated using the tensile strength ratio (TSR), defined in Eq. (16):

$$TSR = \frac{ITS_{Conditioned}}{ITS_{Unconditioned}} \times 100 \tag{16}$$

The indirect tensile strengths of the conditioned and unconditioned samples are denoted as ITS<sub>Conditioned</sub> and ITS<sub>Unconditioned</sub>, respectively. The maximum load applied on the sample is represented by P, while the diameter and thickness of the sample are indicated by d and t, respectively.

#### 3. Results and discution

This section first examines the potential of the bitumen modification process by Nano-ZnO and SBS to produce asphalt with high modulus. After that, the results of the low-, intermediate-, and high-temperature performance of control and modified bitumen will be investigated throughout the BBR, LAS, and MSCR tests. Then, the mixture performance of the moisture susceptibility and low-temperature cracking will be assessed. In addition, a statistical analysis of low-temperature cracking resistance will be performed for bitumen and mixture. A comparison approach is desired to make this analysis. Moreover, the effect of modifiers and their different dosage on the other performances of bitumen and mixture will be studied from a statistical point of view.

#### 3.1. HMAM verification

The dynamic modulus test results at temperature 15°C and frequency 10 Hz for different asphalt mixtures are shown in Fig. 4. According to French specification [37] and the limit of 14000 MPa for the definition of HMAM, this threshold is shown with a red line in Fig. 4.

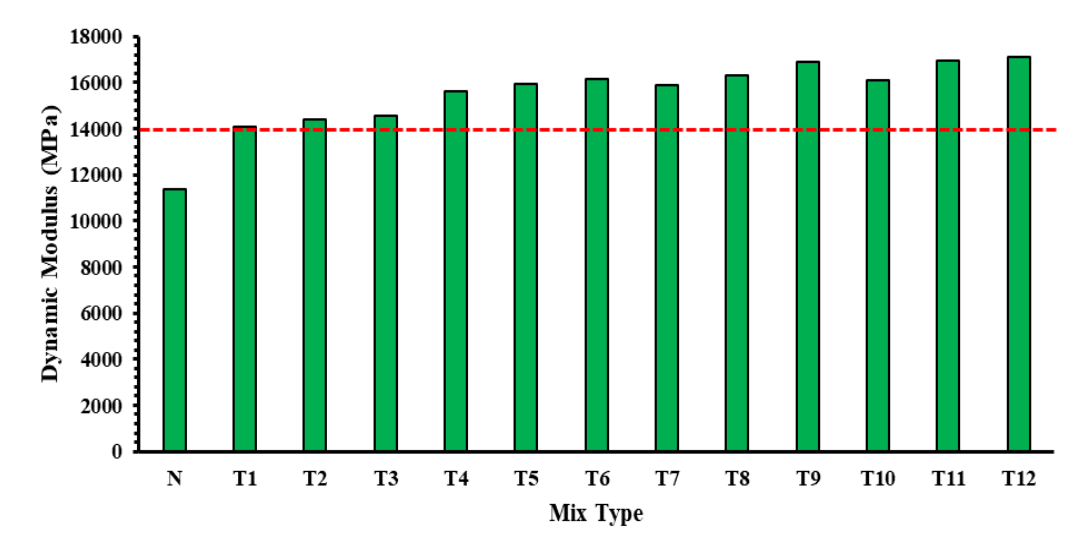


Fig. 4. The results of E\* at test temperature of 15°C and frequency of 10 Hz.

According to the results of E\* in the Fig. 4, it can be said that the control asphalt mixture (N) could not reach the defined threshold for HMAM. However, the modification of bitumen with additives Nano-ZnO and SBS was able to surpass this threshold, resulting in significant dynamic modulus in some samples, such as T6, T9, T11, and T12. Therefore, the hypothesis that bitumen 60/70 can meet the requirements for producing high-modulus asphalt mixtures similar to low-penetration grade bitumen is correct. Consequently, the study proceeded to examine common failures in high-modulus asphalt mixtures to determine whether the use of additives could address typical issues with this type of asphalt, including low-temperature cracking.

## 3.2. Bitumen results

#### 3.2.1. BBR results

The results of the BBR test, i.e., S(t) and m-Value, were determined according to ASTM D6648 standard method. Fig. 5 illustrates the variations of the flexural creep stiffness for different bitumen samples at various temperatures (0°C, -6°C, -12°C, -18°C, -24°C).

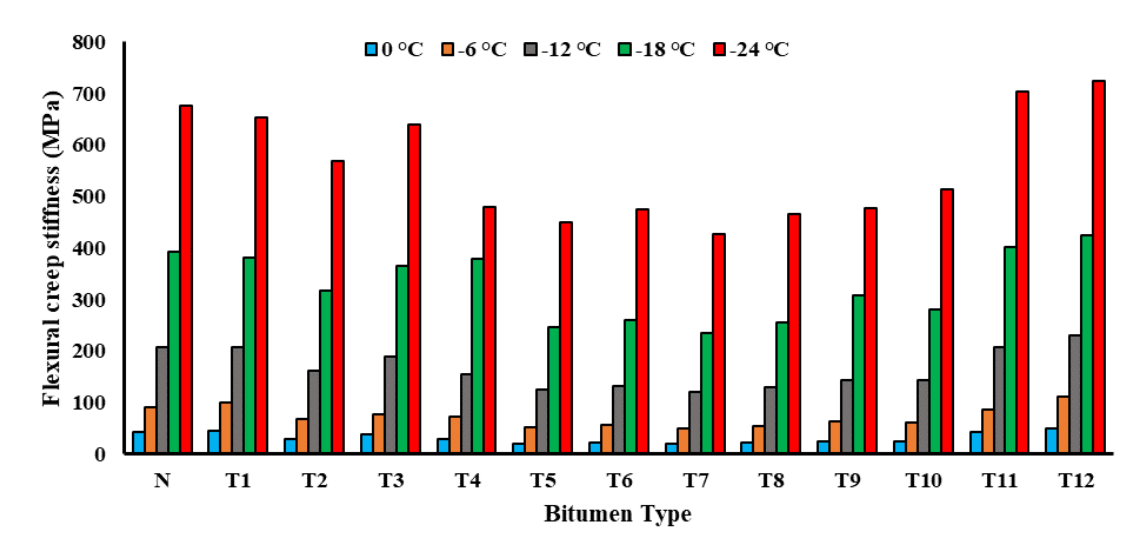


Fig. 5. The results of flexural creep stiffness for different bitumen types at low-temperature.

Based on Fig. 5, it is evident that the flexural creep stiffness increases with the addition of Nano-ZnO Styrene-Butadiene-Styrene. The control sample (N) exhibits the highest stiffness values across all temperatures, indicating poor low-temperature performance. This trend is reversed with the addition of Nano-ZnO, where samples T1 to T3 show decreased stiffness values, indicating improved resistance. Specifically, T2 (4.2% Nano-ZnO) demonstrates the lowest stiffness among Nano-ZnO-only samples, which aligns with the findings of Guo et al. on the benefits of Nano-ZnO in enhancing low-temperature properties [44].

When SBS is incorporated (samples T4 to T12), a further decrease in stiffness is observed. Particularly, T4 up to T10 (4.9% Nano-ZnO and 3.2% SBS) shows the lowest stiffness values, indicating superior low-temperature performance and resistance. A reverse trend can be seen for T11 and T12. These bitumen types show lower resistance potential than control samples at low-temperature. Nevertheless, the combination of Nano-ZnO and SBS makes synergistic improvements in the low-temperature cracking resistance. Specifically, the combination of 4.2% Nano-ZnO and 3.7% SBS in sample T7 is identified as optimal, providing the best performance under low-temperature conditions. This corroborates Zhang et al. [45], who highlighted the positive effects of polymer modifications (Nano-ZnO and SBS) on bitumen properties. In general, based on the results obtained for flexural creep stiffness at five different temperatures, the optimum T7 sample has improved the performance of the HMAM by about 80% compared to the control sample.

The m-value chart, Fig. 6, shows the variations for different bitumen samples at the same temperature range.

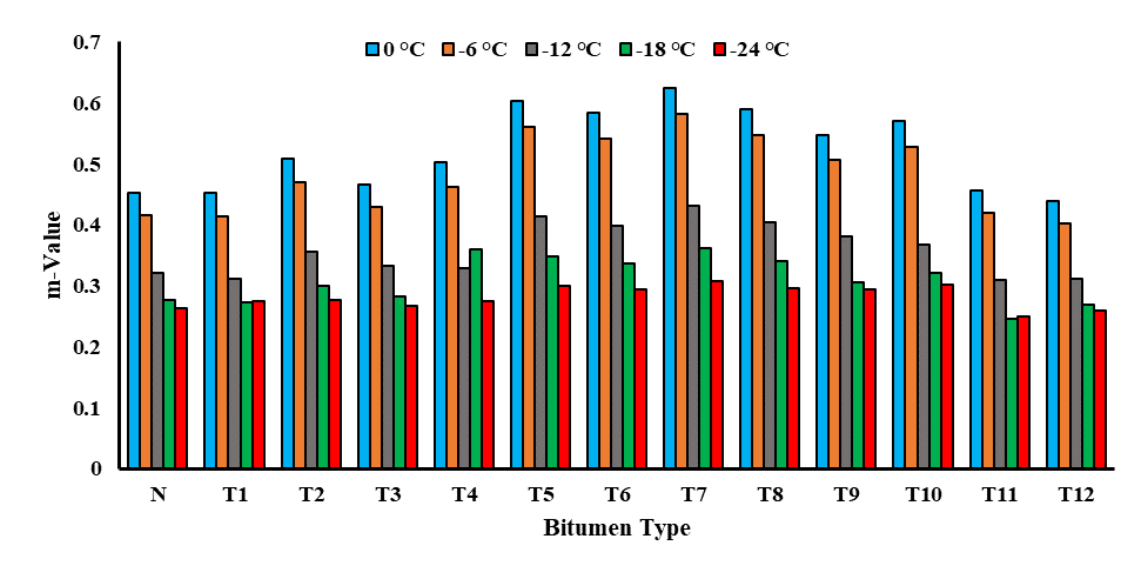


Fig. 6. The results of m-Value for different bitumen types at low-temperature.

The m-value indicates the flexibility and low-temperature performance of bitumen, with higher values indicating better performance. As the temperature decreases from 0°C to -24°C, the m-values for all bitumen types decline, illustrating increased brittleness and reduced flexibility at lower temperatures.

At 0°C, the bitumen types exhibit higher m-values, reflecting better performance in higher temperatures. Conversely, at -24°C, the m-values for all bitumen types reach their lowest points. Notably, some bitumen types (such as T6 and T7) perform better than others (like T10 and T12) across the temperature range. Specifically, bitumen types T5, T6, T7, and T9 maintain relatively higher m-values at lower temperatures, indicating superior performance in cold conditions, whereas types N, T10, and T12 exhibit lower m-values, signifying poorer performance in such conditions.

According to these results, the addition of 3.5% of Nano-ZnO to the control sample increases the m-value, enhancing the material's ability to relax stresses. The optimum dose of Nano-ZnO can be found at 4.2% among T1 to T3. This trend is also generally observed in various combinations with SBS at different temperatures. However, at high dosages of Nano-ZnO and SBS, i.e., T11 and T12, the bitumen modification revealed undesired results. Based on the m-value indicator, T7 (4.2% Nano-ZnO and 3.2% SBS) exhibits the highest m-value, indicating the best relaxation properties and resistance to low-temperature cracking. This observation aligns with the findings of Xie et al. [21], who noted that according to the orthogonal analysis, Nano-ZnO exerts a highly significant influence on the performance of the Nano-ZnO/SBS composite-modified bitumen at both low and high temperatures. Based on the results obtained for m-value at five different temperatures, the optimum T7 sample has improved by about 31% in HMAM performance compared to the control sample. While this improvement was 80% based on the results of flexural creep stiffness. Therefore, it can be generally said that at least 30% of the low-temperature performance of HMAM is improved by 60/70 bitumen modification.

#### 3.2.2. LAS results

The LAS test was conducted on various bitumen types to investigate the fatigue performance of those bitumen at an intermediate temperature of 25°C using DSR, according to AASHTO-TP-101-14 at PAV condition. VECD theory was applied to obtain the related parameters of fatigue performance. The damage parameter of  $\alpha$  is provided for these bitumen types in Fig. 7:

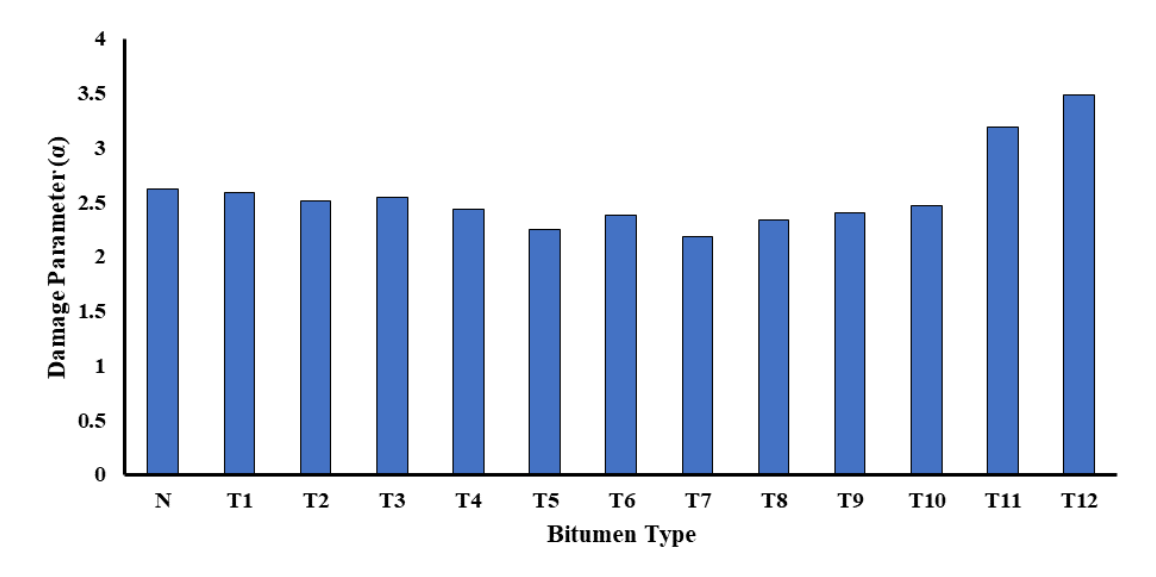


Fig. 7. The damage parameter of different bitumen types obtained based on the VECD theory.

The provided values of the damage parameter  $\alpha$  for various bitumen samples indicate how quickly each sample deteriorates under repeated loading. A higher  $\alpha$  value implies a faster rate of damage. The control sample (N) has an  $\alpha$  value of 2.62, suggesting a moderate rate of damage. Among the samples with only Nano-ZnO (T1 to T3), the  $\alpha$  values are slightly lower than the control sample, with T2 (4.2% Nano-ZnO) having the lowest  $\alpha$  at 2.51, indicating an improved resistance to damage compared to the control.

On the other hand, samples T11 and T12, with higher percentages of Nano-ZnO and SBS, exhibit significantly higher  $\alpha$  values of 3.19 and 3.48, respectively. This indicates that these samples deteriorate much faster, suggesting that there is an optimal range for the addition of Nano-ZnO and SBS beyond which the performance may degrade.

Also, the fatigue curve of control and modified bitumen are shown in Fig. 8, which includes different parameters of  $I_D$ ,  $\alpha$ ,  $C_0$ ,  $C_1$ ,  $C_2$ ,  $D_f$ , k, b, and A, presented in section Bending beam rheometer test.

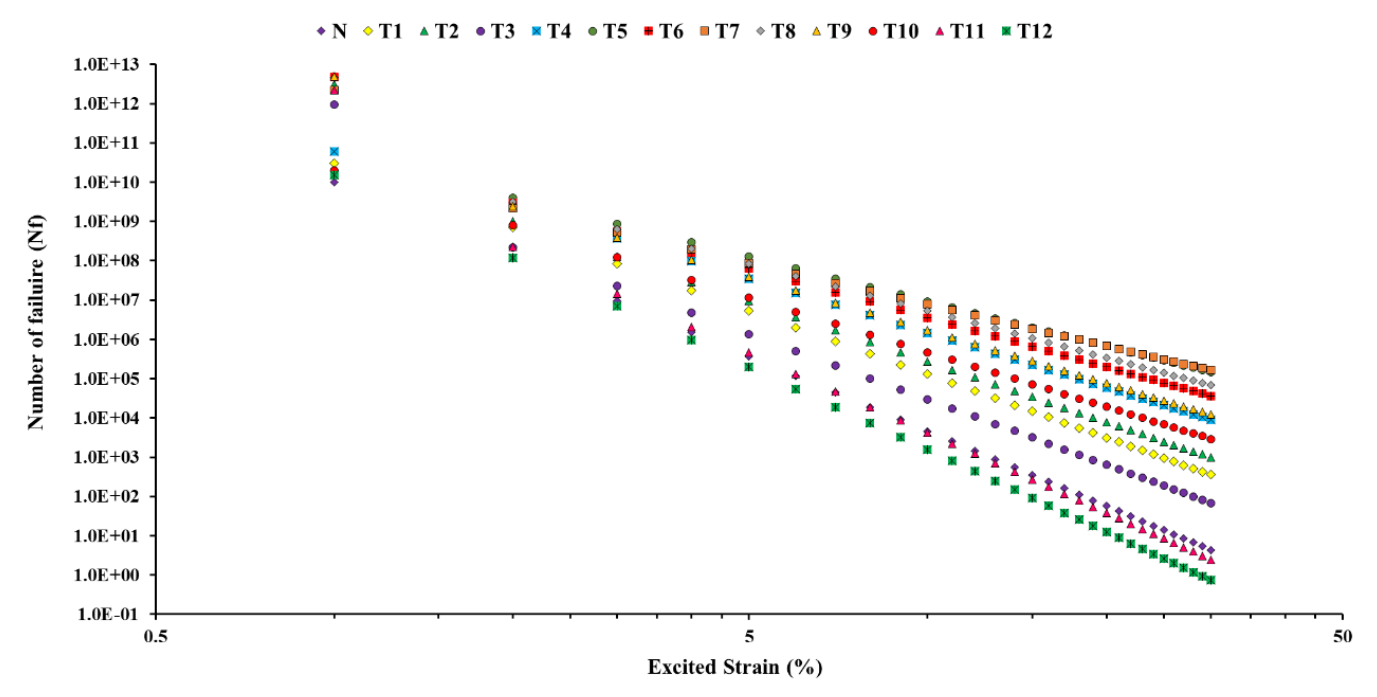


Fig.8. The fatigue curve of different bitumen types at 25°C.

This Fig. 8 illustrates the number of failures relative to excited strain for various bitumen samples. The results reveal that the addition of Nano-ZnO and SBS (Styrene-Butadiene-Styrene) significantly enhances the performance of the asphalt. The control sample (N) without any additives exhibits the lowest number of failures across all strain levels, indicating its poor resistance and performance. In the samples with only Nano-ZnO (T1 to T3), the introduction of Nano-ZnO increases the fatigue life, increasing Nano-ZnO content from 3.5% to 4.9%, further improving bitumen's resistance. This improvement is consistent with the work of Xu et al. [46], who found that modified bitumen with an appropriate amount of Nano-ZnO notably shows more fatigue life than that of unmodified bitumen. When SBS is added to the modified bitumen (T4 to T10), a remarkable increase in the number of failures is observed. The high dosage of Nano-ZnO and SBS shows an inverse trend for fatigue performance. Specifically, across more than 5% strain levels, the sample with 4.9% Nano-ZnO and 4.2% SBS (T12) demonstrates the lowest number of failures, indicating worse resistance and performance. This suggests that while Nano-ZnO alone improves performance, the combination with SBS, particularly at higher percentages, provides the undesired results, corroborating the findings of Zhang et al. on the synergistic effects of polymer modification with different multi-dimensional nanomaterials in bitumen [25].

Moreover, based on the results of Fig. 8, the information of fatigue Eq. (10), i.e., Eq. (11), is derived for each bitumen type and presented in Table 3:

<b>Table 5.</b> Information of rangue Eq. $(N_f - A^{\gamma}_{max})$ for each old inherity per													
Sample Code	N	T1	<b>T2</b>	Т3	<b>T4</b>	T5	<b>T6</b>	<b>T7</b>	T8	Т9	T10	T11	T12
Fatigue oefficients  -B	9	31	35	11	59	55	52	26	49	54	21	24	14
Fati	6.34	5.36	5.11	5.53	4.62	3.77	4.17	3.51	3.97	4.51	4.63	6.78	6.98

**Table 3.** Information of fatigue Eq.  $(N_f = A \times \gamma_{max}^{-B})$  for each bitumen type.

The control sample (N), without any additives, shows the lowest fatigue resistance, indicated by a low A value and a high negative B value, reflecting its poor performance under strain. For samples containing only Nano-ZnO (T1 to T3), the addition of Nano-ZnO enhances fatigue life, with the best performance seen in T2 (4.2% Nano-ZnO), which has the highest A value and a relatively low negative B value. When SBS is added to the bitumen (T4 to T10), a significant increase in fatigue life is observed. Specifically, sample T7 (4.2% Nano-ZnO + 3.2% SBS) and sample T5 (3.5% Nano-ZnO + 3.7% SBS) show the highest fatigue life, with high A values and the least negative B values, indicating superior resistance to fatigue. It is worth mentioning that according to this mathematical Equation, for a given applied strain, the higher the value of parameter A and the lower the absolute value of parameter B, the higher the number of cycles the bitumen can withstand. Moreover, based on the results of Fig. 8 and the mathematical Equation, the influence of parameter B on the obtained fatigue life is greater than that of parameter A. These results are consistent with findings by the damage parameter of  $\alpha$ , demonstrating that Nano-ZnO and SBS can enhance the fatigue resistance properties of bitumen.

#### 3.2.3. MSCR results

Two main results of the MSCR test, i.e., J<sub>nr</sub> and R%, were obtained for different types of bitumen at three temperatures of 58°C, 64°C, and 70°C. Fig.s 9 and 10 represent the J<sub>nr</sub> and R%, respectively, at two stress levels of 0.1 and 3.2 kPa.

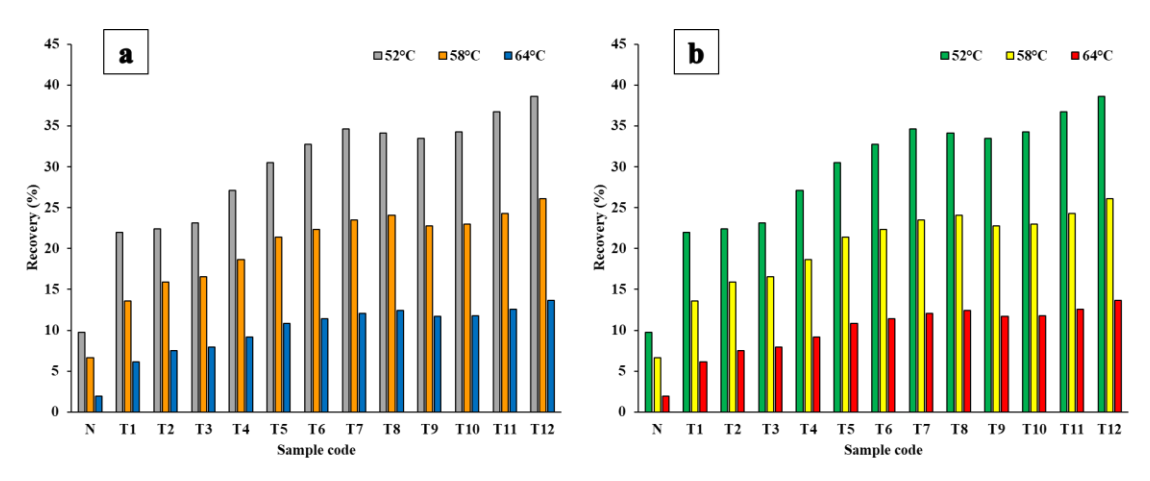
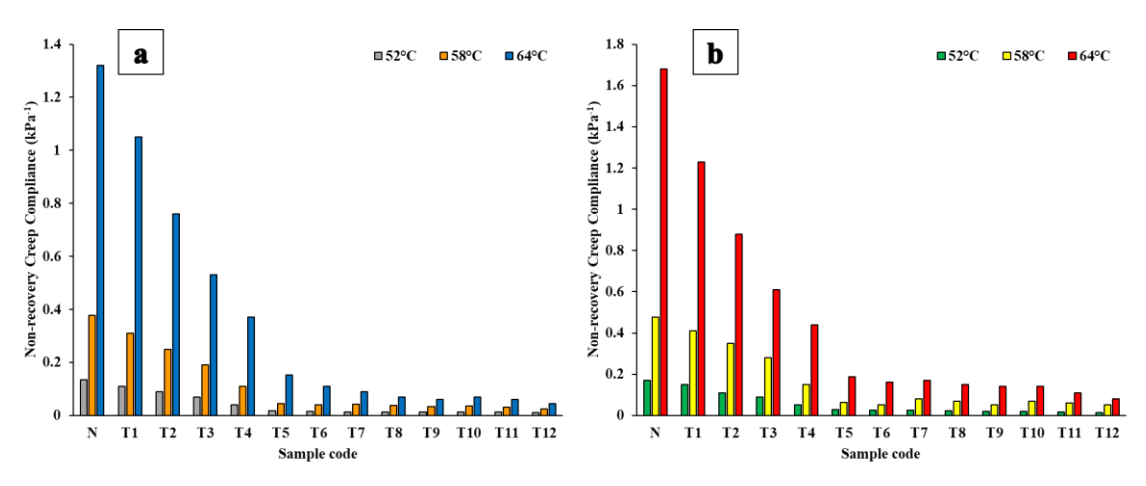


Fig. 9. Recovery percentage of different bitumen types at a) 0.1 kPa and b) 3.2 kPa.



**Fig. 10.** The results of  $J_{nr}$  of different bitumen types at a) 0.1 kPa and b) 3.2 kPa.

The MSCR test results for 0.1 kPa stress level indicate that the addition of Nano-ZnO and SBS significantly influences the performance of the bitumen samples. The recovery percentage in Fig. 8 increases progressively with the inclusion of Nano-ZnO and SBS, showing enhanced elastic recovery. Specifically, samples T4 to T12, which contain both Nano-ZnO and SBS, exhibit substantially higher R% values compared to the samples, i.e., N and samples T1 to T3 with only Nano-ZnO. This demonstrates that the combination of Nano-ZnO and SBS effectively enhances the elastic properties of the bitumen. Previous studies such as Zhang et al. [45] and Neto et al. [47] proved the same conclusion for modified bitumen with Nano-ZnO and SBS.

The non-recoverable creep compliance (J<sub>nr</sub>) values in Fig. 10 decrease with the addition of Nano-ZnO and SBS, indicating improved resistance to permanent deformation. The lowest J<sub>nr</sub> values are observed in samples T11 and T12, signifying that these formulations provide the best resistance to rutting under low-stress conditions. At the higher stress level of 3.2 kPa, the trend observed in the MSCR test results is consistent with that at 0.1 kPa. The R% values are significantly higher for samples with both Nano-ZnO and SBS (T4 to T12) compared to the control sample and samples with only Nano-ZnO. This indicates that the combined additives not only improve elastic recovery at lower stress levels but also maintain their effectiveness under higher stress conditions. Conversely, the J<sub>nr</sub> values remain lower for the modified samples, with T11 and T12 again showing the lowest values. This suggests that the combination of 4.9% Nano-ZnO and 4.2% SBS provides superior performance in terms of both elastic recovery and resistance to permanent deformation. Meanwhile, in the previous performance test results, i.e., low-temperature and

fatigue tests, the two bitumen types of T11 and T12 degraded the performance of the modified bitumen, but they had a positive effect at high temperatures.

#### 3.3. Mixture results

# 3.3.1. Semi-circular bending results

The SCB test was performed on the specimens at -20, -15, and -5°C under a constant loading rate of 0.01 mm/s. Fig.s 11 and 12 depict the results of fracture energy and KIC, respectively.

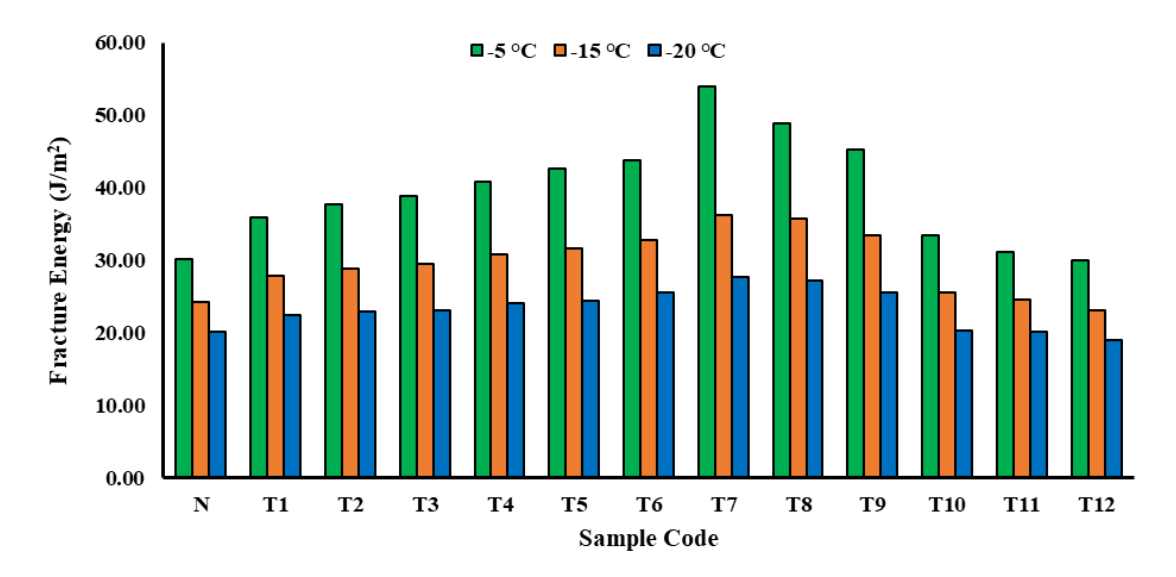


**Fig. 11.** The fracture energy of different asphalt mixtures.

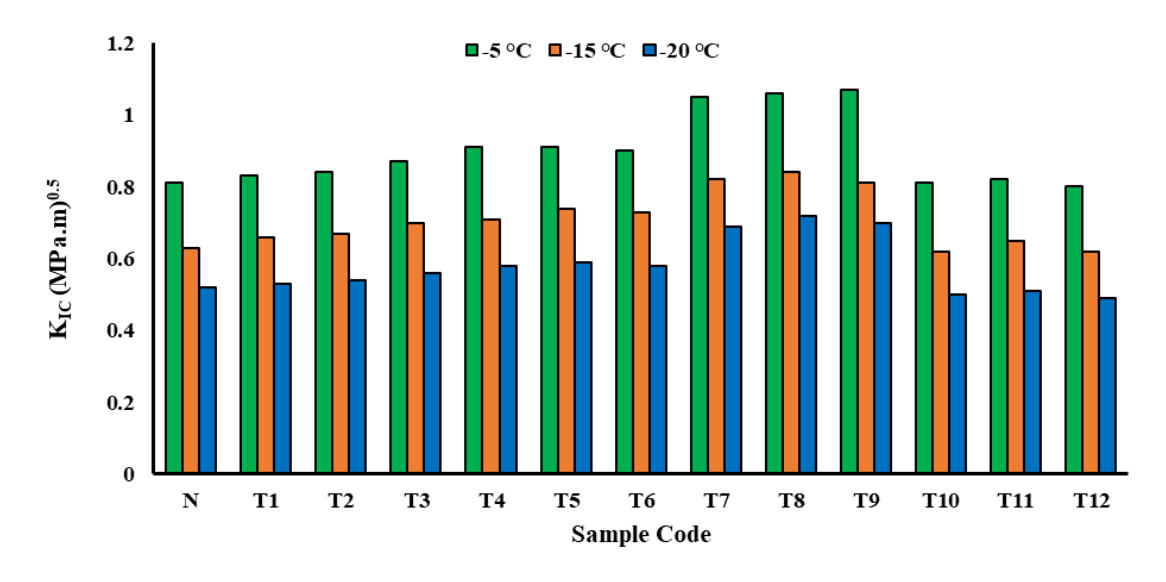


Fig. 12. The results of  $K_{\text{IC}}$  parameter for different asphalt mixtures.

According to Fig. 11, the control sample (N) shows relatively low fracture energy across all temperatures, indicating its lower resistance to fracture compared to modified samples. Using Nano-ZnO and SBS enhances the fracture energy significantly. For instance, samples T6 (3.5% Nano-ZnO and 4.2% SBS) and T7 (4.2% Nano-ZnO and 3.2% SBS) exhibit the highest fracture energy at all temperatures, particularly at -5°C. This suggests that the combination of Nano-ZnO and SBS considerably improves the crack resistance of the asphalt mixtures. The improvement in fracture energy with the addition of Nano-ZnO is consistent with findings by Chen et al. [23], who reported that nanoparticles of Nano-ZnO improve the mechanical performance of asphalt mixtures under low-temperature conditions. Also, according to the

fracture toughness results, samples T6 and T7 display the highest K<sub>IC</sub> values, especially at -5°C, indicating superior fracture toughness. This trend demonstrates that including Nano-ZnO and SBS (up to a certain dosage) not only improves the fracture energy but also enhances the material's ability to resist crack propagation. The results align with the study by Kamboozia et al. [24], which found that polymer-modified asphalt mixtures with Nano-ZnO and SBS exhibit higher fracture toughness. The control sample (N) shows the worst performance across all temperatures. Samples with higher Nano-ZnO and SBS content (like T12 with 4.9% Nano-ZnO and 4.2% SBS) approximately perform similarly to the control sample. However, the positive effect of the modification is more pronounced at lower Nano-ZnO and SBS levels, suggesting an optimal range for maximizing fracture resistance.

# 3.3.2. Moisture durability results

The results of TSR, as the key indicator of the moisture susceptibility of asphalt mixtures, including the control sample (N) and those modified with Nano-ZnO and SBS, are shown in Fig. 13. The red dashed line represents the 80% threshold, which is commonly accepted as the minimum required TSR value for acceptable moisture resistance in asphalt mixtures.

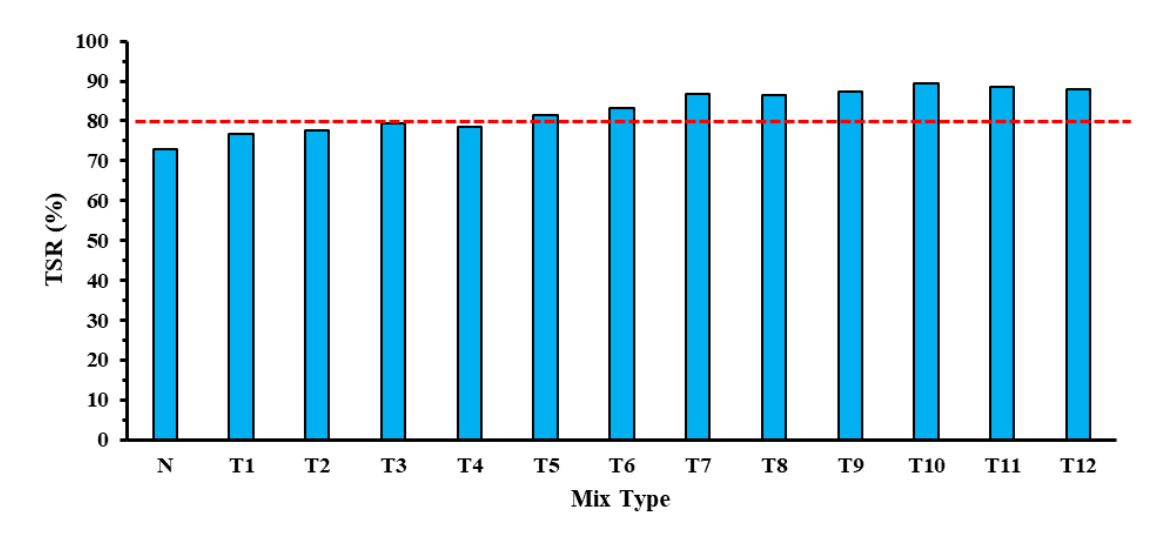


Fig. 13. The result of TSR of different asphalt mixtures.

The control sample (N) shows a TSR value slightly below the 80% threshold, indicating marginal compliance with moisture resistance standards. Samples T1 to T12, which incorporate Nano-ZnO and SBS modifiers, all exhibit TSR values above the 80% threshold, with most samples significantly exceeding this benchmark. Notably, samples T7 (4.2% Nano-ZnO and 3.2% SBS), T10 (4.9% Nano-ZnO and 3.2% SBS), T11 (4.9% Nano-ZnO and 3.7% SBS), and T12 (4.9% Nano-ZnO and 4.2% SBS) demonstrate the highest TSR values, approaching or exceeding 90%. This trend suggests that adding Nano-ZnO and SBS significantly enhances the moisture resistance of asphalt mixtures. Based on these findings and considering the dosage and effectiveness of each additive, Nano-ZnO and SBS, it can be concluded that sample T7 can be selected as the most effective combination for improving moisture resistance in asphalt mixture. The superior performance of these modified samples aligns with findings from previous research. For instance, studies by Chen et al. [23] and Behnood and Gharehveran [48] have shown that polymer-modified asphalts, particularly those incorporating SBS, exhibit improved resistance against damage caused by moisture. The presence of Nano-ZnO further contributes to this improvement, as noted by researchers such as Su et al. [22] and Shi et al. [49], who reported that this nanomaterial improves the overall durability and moisture resistance of asphalt binder. Additionally, the surface free energy method results about the adhesion [50] and cohesion properties [51] of modified bitumen with Nano-ZnO and SBS confirm the above findings.

# 3.4. Statistical analysis

ANOVA analysis, with a 95% confidence interval, is conducted based on the amount of Nano-ZnO and SBS additives to examine their impact on the viscoelastic properties of bitumen and the mechanical properties of the asphalt mixture. Before performing the ANOVA, the Shapiro-Wilk test served to assess whether the data followed a normal distribution, and homoscedasticity (homogeneity of variances) was verified using Levene's test. The results confirmed that the necessary assumptions were met, ensuring the validity of the ANOVA analysis. The ANOVA results, including F-value and P-value parameters and their significance, are presented in Tables 4 and 5 for BBR and SCB tests, respectively. The reason for choosing these two tests is that both are suited for evaluating low-temperature changes and resistance to thermal cracking. Subsequently, ANOVA analysis for the Nano-ZnO and SBS additive variables will be discussed.

**Table 4.** The results of ANOVA analysis for BBR test results.

Dependent Variable	Test Temperature (°C)	Factor	F-value	P-value	Significance
	0	Nano-ZnO	8.54	0.007	Sig.
	0	SBS	15.32	0.002	Sig.
	-	Nano-ZnO	9.02	0.005	Sig.
SS	-6	SBS	13.24	0.003	Sig.
Stiffness	12	Nano-ZnO	7.81	0.009	Sig.
ţţţ	-12	SBS	11.56	0.004	Sig.
$\infty$	10	Nano-ZnO	7.45	0.01	Sig.
	-18	SBS	12.02	0.004	Sig.
	-24	Nano-ZnO	6.78	0.013	Sig.
		SBS	13.89	0.003	Sig.
	0	Nano-ZnO	5.34	0.024	Sig.
		SBS	14.02	0.003	Sig.
	-6	Nano-ZnO	6.12	0.017	Sig.
o		SBS	12.88	0.003	Sig.
alu	12	Nano-ZnO	7.65	0.011	Sig.
m-Value	-12	SBS	11.23	0.005	Sig.
	-18	Nano-ZnO	8.01	0.008	Sig.
		SBS	12.09	0.004	Sig.
	24	Nano-ZnO	7.32	0.01	Sig.
	-24	SBS	11.87	0.004	Sig.

**Table 5.** The results of ANOVA analysis for SCB test results.

Dependent Variable	Test Temperature (°C)	Factor	F-value	P-value	Significance
X:	-5	Nano-ZnO	12.45	0.003	Sig.
energy t)	-3	SBS	14.32	0.002	Sig.
	-15	Nano-ZnO	8.67	0.006	Sig.
Fracture (G	-13	SBS	11.23	0.005	Sig.
act	-20	Nano-ZnO	9.32	0.005	Sig.
$\Pi$		SBS	13.67	0.003	Sig.
	-5	Nano-ZnO	8.78	0.006	Sig.
		SBS	12.45	0.004	Sig.
$K_{ m IC}$	-15	Nano-ZnO	10.45	0.004	Sig.
⊻ _		SBS	15.78	0.002	Sig.
		Nano-ZnO	7.98	0.008	Sig.
	-20	SBS	14.01	0.003	Sig.

Overall, according to ANOVA analysis, Nano-ZnO has a significant impact (P-value less than 0.05) on both BBR and SCB characteristics. This indicates that adding Nano-ZnO leads to significant changes in stiffness and m-Value at various temperatures, as well as in G<sub>f</sub> and K<sub>Ic</sub> parameters at different

difference

temperatures. Similar to Nano-ZnO, SBS also has a significant effect (P-value less than 0.05) on BBR and SCB characteristics. This shows that adding SBS also causes substantial changes in the mechanical and viscoelastic properties of the asphalt mixture. Both Nano-ZnO and SBS factors have similar effects on the studied characteristics. However, in some cases, the impact of SBS seems to be greater than that of Nano-ZnO (based on F-value). In summary, the ANOVA results indicate that both Nano-ZnO and SBS additives improve the mechanical and viscoelastic properties of bitumen and asphalt mixtures at low temperatures, and these effects are significant at various temperatures. In other words, these improvements are due to the use of the two mentioned additives and not due to experimental error.

In addition to the ANOVA analyses presented for evaluating the influence of Nano-ZnO and SBS additives on the mechanical and viscoelastic properties of asphalt mixtures, a comparative statistical assessment was conducted to verify whether modified 60/70 penetration grade bitumen can meet the mechanical performance criteria typically achieved by using low-penetration grade binders (e.g., 10/35). For this purpose, control HMAM specimens were prepared using both conventional low-penetration bitumen and Nano-ZnO/SBS-modified 60/70 bitumen under identical mix designs and testing protocols. Performance metrics, including dynamic modulus (at 25°C and 10 Hz) and moisture resistance (quantified by TSR) were statistically analyzed using independent sample t-tests at a 95% confidence level.

	1 0				
Parameter	Low Penetration Binder	Modified 60/70 Binder (T10)	t-value	P-value	Conclusion
Dynamic Modulus (MPa) @ 25°C and frequency of 10Hz	13520	13260	0.711	0.487	No significant difference
TSR (%)	90	91	0.541	0.598	No significant

**Table 6.** Results of t-test comparing HMAM with low-penetration and modified 60/70 bitumen.

As shown in Table 6, the p-values for both dynamic modulus and TSR value exceed 0.05, indicating no statistically significant difference between the mechanical performance of HMAM produced with low-penetration bitumen and those using modified 60/70 bitumen (T10). Therefore, the hypothesis that modified 60/70 bitumen can effectively replace low-penetration grades for HMAM production is statistically validated.

# 4. Summary and conclusions

This study attempted to use a commonly used bitumen in the road paving industry instead of a bitumen with a low penetration grade to produce high-modulus asphalt mixture (HMAM). Two additives, Nano-ZnO and SBS, were used to achieve the required stiffness and address thermal-cracking issues in HMAM made with low-penetration grade bitumen. After ensuring the production of high-modulus asphalt mixture, other performance tests for bitumen and asphalt mixture were conducted. These tests included BBR, LAS, and MSCR for bitumen, and low-temperature (SCB) and moisture susceptibility tests were performed for the mixture. The results were then discussed, and statistical analysis, using one-way ANOVA, was conducted. In addition to the experimental results, the findings of Su et al. [22] provide molecular-level evidence supporting the observed improvements in the modified asphalt binders used in this study. Through molecular dynamics simulations, Su et al. [22] demonstrated that the incorporation of Nano-ZnO in combination with SBS enhances the molecular structure of asphalt binders by promoting stronger interactions between the nano-particles, SBS polymer chains, and the base bitumen matrix. Their results confirmed that Nano-ZnO not only improves the dispersion of SBS within the bitumen but also

reinforces the nano-scale network structure, leading to increased stiffness and reduced molecular mobility. These mechanisms align with the experimental improvements observed in this study, including increased softening point, reduced penetration, and enhanced resistance to rutting and fatigue. Therefore, the conclusions drawn from this experimental work are consistent with the molecular-level mechanisms identified by Su et al. [22], providing a comprehensive understanding of how Nano-ZnO/SBS modifiers improve the overall performance of asphalt binders. Moreover, several studies have confirmed the effectiveness of nanomaterials through molecular dynamics simulations, demonstrating their potential in enhancing the molecular structure and mechanical properties of composite materials [16,52,53], A summary of the results of the current study and the corresponding reasons are presented as follows:

- According to the aggregate packing theory, using the gap-graded asphalt mixture did not generate HMAM. While using Nano-ZnO and SBS additives, HMAM was produced, and in some cases, significant improvement in dynamic modulus was achieved.
- Nano-ZnO and SBS significantly enhance the physical properties of bitumen [41]. Nano-ZnO reduces the solubility parameter of asphalt, improving compatibility with SBS, and increases the elastic, bulk, and shear moduli of the asphalt. These results align with experimental findings showing that the optimal blend of 4.2% Nano-ZnO and 3.2% SBS (T7) offers improved low-temperature performance, increased flexural creep stiffness, and m-value.
- Nano-ZnO and SBS improve the damage resistance and fatigue performance of bitumen. The optimal combination for intermediate-cracking resistance is 4.2% Nano-ZnO and 3.2% SBS, demonstrating enhanced durability under high strain. The molecular dynamics results corroborate these findings by showing that the presence of Nano-ZnO and SBS minimizes the buildup of highly polar compounds and improves the structural arrangement of the bitumen [41], thus improving durability and fatigue resistance.
- Nano-ZnO and SBS significantly improve elastic recovery and reduce non-recoverable creep compliance. The optimal blend, T12 (4.9% Nano-ZnO and 4.2% SBS), shows superior performance in these parameters, indicating enhanced resistance to both elastic and permanent deformations.
- Adding Nano-ZnO and SBS enhances the fracture properties of asphalt mixture, increasing resistance to low-temperature cracking. Additionally, the modifications improve moisture resistance, with higher TSR values indicating better performance in moisture-prone environments, thus extending the lifespan and performance of asphalt pavements. The surface free energy method results about the adhesion and cohesion properties of modified bitumen with Nano-ZnO and SBS confirm the above findings.
- Overall, the literature's molecular dynamics study and the current study confirm the positive impact of Nano-ZnO and SBS on improving the physical properties, molecular structure, and performance of bitumen and mixture. The optimum percentages of Nano-ZnO and SBS can be suggested as 4.2% and 3.2%, respectively. These findings highlight the significant benefits of these additives in improving the longevity of asphalt mixtures.

The synergistic improvement of bitumen properties through the combined use of Nano-ZnO and SBS can be attributed to their complementary mechanisms at both micro- and molecular scales. SBS enhances the elasticity and deformation resistance by forming a three-dimensional polymer network within the bitumen matrix. Meanwhile, Nano-ZnO particles, due to their high surface area and nano-scale dispersion, interact with both the bitumen and the polymer phase, leading to improved stiffness, thermal stability, and aging resistance. Similar synergistic effects of nanomaterials in modified bituminous composites have been demonstrated in previous studies [54–57], where nano-reinforcements enhanced the structural integrity of polymer matrices.

Comparing the present results with prior research, the improvement in stiffness and fracture resistance observed with Nano-ZnO/SBS modification aligns with the trends reported by Su et al. [22], who highlighted the role of Nano-ZnO in strengthening asphalt at the molecular level. However, unlike studies focusing solely on bitumen performance, this work extends these findings to HMAM mixtures, emphasizing their practical application under demanding load conditions.

# **Future Research Directions**

Future studies are recommended to validate the laboratory results of modified HMAM containing 60/70 bitumen through large-scale field trials under various climatic and loading conditions. In addition, advanced characterization techniques such as SEM and FTIR should be utilized to provide deeper insight into the microstructural interactions between Nano-ZnO, SBS, and the bitumen matrix. Investigating the long-term aging behavior, moisture susceptibility, and durability of these modified mixtures for different freezing-thaw cycles will also contribute to their practical application. Furthermore, exploring other nanomaterials or sustainable additives may enhance both performance and environmental benefits in high-modulus asphalt technologies.

# **Funding**

This research did not receive any specific grant from funding agencies in the public, commercial, or not-for-profit sectors.

# **Conflicts of Interest**

The author (Gh. Shafabakhsh) is an Editorial Board Member for Journal of Rehabilitation in Civil Engineering and was not involved in the editorial review or the decision to publish this article.

# **Authors' Contribution Statement**

**Shahram Naseri**: Conceptualization; Data curation; Formal analysis; Investigation; Methodology; Resources; Software; Validation; Visualization; Roles/Writing – original draft; Writing – review & editing.

**Gholamali Shafabakhsh:** Conceptualization; Project administration; Resources; Supervision; Validation; Visualization; Writing – review & editing.

Alireza Khavandi: Conceptualization; Supervision; Writing – review & editing.

#### References

- [1] Mahpour A, Khodadadi M, Moghadas Nejadd F. Investigation the Moisture Susceptibility of Warm-Mix Asphalt Modified with Nano-TiO2 and Waste Rubber Granules. J Transp Res 2023;20:55–70.
- [2] Nejad FM, Noory A, Khodadadi M. The shear bonding of interlayer's effect on rutting parameters of an asphalt overlay. Geosynth. Lead. W. to a Resilient Planet, CRC Press; 2023, p. 1233–40.
- [3] Khodadadi M, Azarhoosh A, Moghaddas Nejad F, Khodaii A. Investigation of the Moisture Susceptibility of Nanocomposite-Modified Asphalt Mixture Using Surface Free Energy Theory. AUT J Civ Eng 2021;5:287–300.
- [4] Khodadadi M, Moradi L, Dabir B, Nejad FM, Khodaii A. Reuse of drill cuttings in hot mix asphalt mixture: A study on the environmental and structure performance. Constr Build Mater 2020;256:119453.
- [5] Petho L, Beecroft A, Griffin J, Denneman E. High modulus high fatigue resistance asphalt (EME2) technology transfer. 2014.

- [6] Petho L, Bryant P. High modulus asphalt (EME2) pavement design in Queensland. AAPA Int. Flex. Pavements Conf. 16th, 2015, Gold Coast, Queensland, Aust., 2015.
- [7] Olard F, Dherbecourt J, Dumont H. GB5: Eco-friendly alternative to EME2 for long-life and cost-effective base courses. Eur Roads Rev 2012.
- [8] Olard F, Perraton D. On the optimization of the aggregate packing for the design of self-blocking high-performance asphalts. Congr. Int. Soc. Asph. Pavements, Nagoya, vol. 5, 2010.
- [9] Gajewski M, Bańkowski W, Pronk AC. Evaluation of fatigue life of high modulus asphalt concrete with use of three different definitions. Int J Pavement Eng 2020;21:1717–28.
- [10] Petho L, Bryant P, Jones J, Denneman E. EME2 pavement and mix design. Road Transp Res A J Aust New Zeal Res Pract 2016;25:3–14.
- [11] Denneman E, Petho L, Verhaeghe BMJA, Komba JJ, Steyn W, Vos R, et al. High modulus asphalt (EME) technology transfer to South Africa and Australia: shared experiences 2015.
- [12] Khodadadi M, Khodaii A, Absi J, Hajikarimi P, Tehrani FF. Multi-Length-Scale Investigation of the Fatigue Behavior of Bituminous Composites, I: Experimental Approach. J Mater Civ Eng 2024. https://doi.org/10.1061/JMCEE7/MTENG-19135.
- [13] Khodadadi M, Khodaii A, Absi J, Tehrani FF, Hajikarimi P. An experimental length scale investigation on viscoelastic behavior of bituminous composites: Focusing on mortar scale. Constr Build Mater 2021;308:124766. https://doi.org/https://doi.org/10.1016/j.conbuildmat.2021.124766.
- [14] Diefenderfer BK, Maupin Jr GW. Field trials of high-modulus high-binder-content base layer hot-mix asphalt mixtures. 2010.
- [15] Pouget S, Olard F, Hammoum F. GB5®mix design: a new approach for aggregate grading optimization for heavy duty flexible pavements. 8th RILEM Int. Conf. Mech. Crack. Debonding Pavements, 2016, p. 17–23.
- [16] Mangiafico S, Sauzéat C, Di Benedetto H, Pouget S, Olard F, Planque L, et al. Statistical analysis of influence of mix design parameters on mechanical properties of mixes with reclaimed asphalt pavement. Transp Res Rec 2014;2445:29–38.
- [17] Lee HJ, Lee JH, Park HM. Performance evaluation of high modulus asphalt mixtures for long life asphalt pavements. Constr Build Mater 2007;21:1079–87.
- [18] Moreno-Navarro F, Sol-Sánchez M, Tomás-Fortún E, Rubio-Gámez MC. High-modulus asphalt mixtures modified with acrylic fibers for their use in pavements under severe climate conditions. J Cold Reg Eng 2016;30:4016003.
- [19] Mahpour A, Khodadadi M, Shahraki M, Moghadas Nejad F. Evaluation of Moisture Durability of Modified Asphalt Mixture with Nano-Titanium Dioxide Using Surface Free Energy Method. Amirkabir J Civ Eng 2022;54:2831–50. https://doi.org/https://doi.org/10.22060/ceej.2021.19458.7180.
- [20] Khodadadi M, Moghadas Nejad F, Khodaii A. Comparison of Rut Susceptibility Parameters in Modified Bitumen with PPA. AUT J Civ Eng 2017;1:129–34.
- [21] Xie X, Hui T, Luo Y, Li H, Li G, Wang Z. Research on the Properties of Low Temperature and Anti-UV of Asphalt with Nano-ZnO/Nano-TiO2/Copolymer SBS Composite Modified in High-Altitude Areas. Adv Mater Sci Eng 2020;2020:9078731.
- [22] Su M, Si C, Zhang Z, Zhang H. Molecular dynamics study on influence of Nano-ZnO/SBS on physical properties and molecular structure of asphalt binder. Fuel 2020;263:116777.
- [23] Chen X, Wen P, Ji Q, Jiang S, Zhou Z, Wang A, et al. Adhesion of Nano-ZnO Modified Asphalt and Its Influence on Moisture-Sensitive Properties of Mixtures. Adv Mater Sci Eng 2023;2023:8888248.
- [24] Kamboozia N, Rad SM, Saed SA. Laboratory Investigation of the Effect of Nano-ZnO on the Fracture and Rutting Resistance of Porous Asphalt Mixture under the Aging Condition and Freeze Thaw Cycle 2022;34:1–17. https://doi.org/10.1061/(ASCE)MT.1943-5533.0004187.
- [25] Zhang D, Chen Z, Zhang H, Wei C. Rheological and anti-aging performance of SBS modified asphalt binders with different multi-dimensional nanomaterials. Constr Build Mater 2018;188:409–16.
- [26] AASHTO PP. The laboratory evaluation of modified asphalt systems. Am Assoc State Highw Transp Off 1993.
- [27] Ghanizadeh AR. An optimization model for design of asphalt pavements based on IHAP code number 234. Adv Civ Eng 2016;2016:5942342.

- [28] M.M. Design, Marshall Mix Design 26.1, NPTEL May 24. (2006) 1–7. n.d.
- [29] Astm D. 2872: Standard test method for effect of heat and air on a moving film of asphalt (rolling thin-film oven test). Am Soc Test Mater West Conshohocken, PA 2012.
- [30] Test O. Accelerated aging of asphalt binder using a pressurized aging vessel (PAV) 2012.
- [31] ASTM D. Standard test method for determining the flexural creep stiffness of asphalt binder using the bending beam rheometer (BBR), 2008.
- [32] Timoshenko S. Elementary theory and problems. Van Nostrand; 1940.
- [33] Liu S, Cao W, Shang S, Qi H, Fang J. Analysis and application of relationships between low-temperature rheological performance parameters of asphalt binders. Constr Build Mater 2010;24:471–8.
- [34] Zeng Z 'Alan,' Underwood BS, Castorena C. Low-temperature performance grade characterisation of asphalt binder using the dynamic shear rheometer. Int J Pavement Eng 2022;23:811–23.
- [35] Test FO. Estimating damage tolerance of asphalt binders using the linear amplitude sweep. AASHTO TP 2010:101–14.
- [36] AASHTO T. Standard method of test for determining dynamic modulus of hot-mix asphalt (HMA). Am Assoc State Highw Transp Off Washington, DC 2011;444.
- [37] Capitão S, Picado-Santos L. Applications, properties and design of high modulus bituminous mixtures. Road Mater Pavement Des 2006;7:103–17.
- [38] Lim IL, Johnston IW, Choi SK, Boland JN. Fracture testing of a soft rock with semi-circular specimens under three-point bending. Part 1—mode I. Int. J. rock Mech. Min. Sci. Geomech. Abstr., vol. 31, 1994, p. 185–97.
- [39] Li X, Marasteanu M. The fracture process zone in asphalt mixture at low temperature. Eng Fract Mech 2010;77:1175–90.
- [40] Recommendation RD. Determination of the fracture energy of mortar and concrete by means of three-point bend tests on notched beams. Mater Struct 1985;18:285–90.
- [41] Shafabakhsh G, Sadeghnejad M, Ebrahimnia R. Fracture resistance of asphalt mixtures under mixed-mode I/II loading at low-temperature: Without and with nano SiO2. Constr Build Mater 2021;266:120954. https://doi.org/https://doi.org/10.1016/j.conbuildmat.2020.120954.
- [42] Aragao FTS, Kim Y-R. Characterization of fracture properties of asphalt mixtures based on cohesive zone modeling and digital image correlation technique. 2011.
- [43] AASHTO T. 283 Resistance of Compacted Bituminous Mixture to Moisture Induced Damage. Am Assocation State Hishw Transp Off 1998.
- [44] Guo G, Zhang H. The effect of morphology of ZnO particle on properties of asphalt binder and mixture. Int J Transp Sci Technol 2022;11:437–54.
- [45] Zhang H, Su M, Zhao S, Zhang Y, Zhang Z. High and low temperature properties of nano-particles/polymer modified asphalt. Constr Build Mater 2016;114:323–32.
- [46] Xu X, Guo H, Wang X, Zhang M, Wang Z, Yang B. Physical properties and anti-aging characteristics of asphalt modified with nano-zinc oxide powder. Constr Build Mater 2019;224:732–42.
- [47] Duan H, Zhang H, Lv S, Lu W, Ge D, Jiang R, et al. Revealing aging behavior retarding mechanism of zinc oxide/expanded vermiculite composite modified bituminous mixture. Constr Build Mater 2025;468:140388.
- [48] Behnood A, Gharehveran MM. Morphology, rheology, and physical properties of polymer-modified asphalt binders. Eur Polym J 2019;112:766–91.
- [49] Shi X, Goh SW, Akin M, Stevens S, You Z. Exploring the interactions of chloride deicer solutions with nanomodified and micromodified asphalt mixtures using artificial neural networks. J Mater Civ Eng 2012;24:805–15.
- [50] Esmaeili N, Hamedi GH, Khodadadi M. Determination of the stripping process of asphalt mixtures and the effective mix design and SFE parameters on its different phases. Constr Build Mater 2019;213. https://doi.org/10.1016/j.conbuildmat.2019.04.043.
- [51] Khodadadi M, Azarhoosh A, Khodaii A. Influence of polymeric coating the aggregate surface on moisture damage of hot mix asphalt. Period Polytech Civ Eng 2021;65:376–84. https://doi.org/https://doi.org/10.3311/PPci.14340.

- [52] Angili SN, Morovvati MR, Kardan-Halvaei M, Saber-Samandari S, Razmjooee K, Abed AM, et al. Fabrication and finite element simulation of antibacterial 3D printed Poly L-lactic acid scaffolds coated with alginate/magnesium oxide for bone tissue regeneration. Int J Biol Macromol 2023;224:1152–65.
- [53] Qian WM, Vahid MH, Sun YL, Heidari A, Barbaz-Isfahani R, Saber-Samandari S, et al. Investigation on the effect of functionalization of single-walled carbon nanotubes on the mechanical properties of epoxy glass composites: Experimental and molecular dynamics simulation. J Mater Res Technol 2021;12:1931–45. https://doi.org/10.1016/j.jmrt.2021.03.104.
- [54] Office JE, Chen J, Dan H, Ding Y, Gao Y, Guo M, et al. New innovations in pavement materials and engineering: A review on pavement engineering research 2021. J Traffic Transp Eng (English Ed 2021;8:815–999.
- [55] Khodadadi M, Khodaii A, Hajikarimi P, Fakhari Tehrani F, Absi J. Multi-Scale Numerical Viscoelastic Simulation of Fatigue Behavior of Asphalt Mixtures Modified with Polyphosphoric Acid. IOP Conf. Ser. Mater. Sci. Eng., vol. 416, 2018. https://doi.org/10.1088/1757-899X/416/1/012106.
- [56] Hamedi GH, Azarhoosh AZ, Khodadadi M. Effects of asphalt binder modifying with polypropylene on moisture susceptibility of asphalt mixtures with thermodynamically concepts. Period Polytech Civ Eng 2018;62. https://doi.org/10.3311/PPci.11570.
- [57] Mahpour A, Alipour S, Khodadadi M, Khodaii A, Absi J. Leaching and mechanical performance of rubberized warm mix asphalt modified through the chemical treatment of hazardous waste materials. Constr Build Mater 2023;366:130184. https://doi.org/https://doi.org/10.1016/j.conbuildmat.2022.130184.